ACS Sustainable Chemistry & Engineering

pubs.acs.org/journal/ascecg

Research Article

Toward the Recycling of Low-GWP Hydrofluorocarbon/Hydrofluoroolefin Refrigerant Mixtures Using Composite Ionic Liquid–Polymer Membranes

Fernando Pardo, Sergio V. Gutiérrez-Hernández, Gabriel Zarca, and Ane Urtiaga*

Cite This: *ACS Sustainable Chem. Eng.* 2021, 9, 7012–7021

Read Online

ACCESS | Metrics & More | Article Recommendations | Supporting Information

ABSTRACT: The restrictions imposed to the production of high-global warming potential refrigerant gases have boosted the search of novel separation processes for the selective recovery of hydrofluorocarbons (HFCs) and hydrofluoroolefins (HFO) from exhausted refrigerant mixtures. Membrane materials functionalized with ionic liquids can offer an effective techno-economical response to the challenging separation of HFC/HFO blends. In this work, we provide for the first time a thorough characterization of the gas solubility and permeation properties of three of the most relevant compounds for the future of the refrigeration and air conditioning sector, that is, difluoromethane (HFC-R32), 1,1,1,2-tetrafluoroethane (HFC-R134a), and 2,3,3,3-tetrafluoropropene (HFO-R1234yf), through composite ionic liquid–polymer membranes (CILPMs) that were prepared combining the Pebax 1657 copolymer with several ILs, [C_2mim][SCN], [C_2mim][BF_4], [C_2mim][OTf], and [C_2mim][Tf_2N], varying the IL content in the range of 20–60 wt %. The CILPMs with the best separation performance and mechanical stability against feed pressure were those with 40 wt % of [C_2mim][BF_4] and [C_2mim][SCN]. For the 40 wt % [C_2mim][BF_4] CILPM, the addition of IL promoted the permeability of the smallest molecules R32 and R134a and reduced the permeability of the largest molecule R1234yf, which resulted in 120 and 75% selectivity enhancement relative to that of the pristine polymer for R32/R1234yf and R134a/R1234yf mixtures, respectively. Finally, this CILPM was stable in the separation of two commercial HFC/HFO refrigerant blends (R513A and R454B) over a wide pressure range (up to 12 bar). These results indicate that CILPMs can be used for separating azeotropic and near-azeotropic exhausted HFC/HFO mixtures, which could stimulate the recovery and reuse of their components and thus avoid their emissions and pull down the demand for virgin refrigerants.

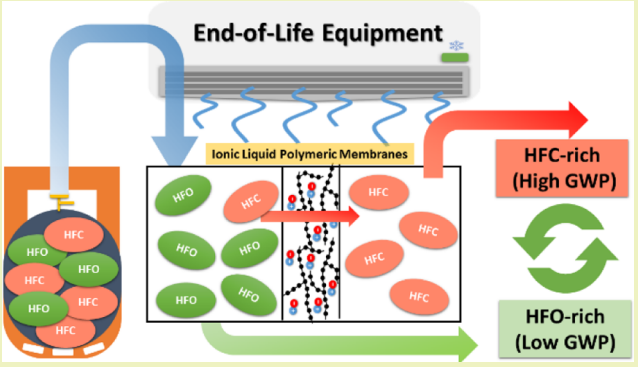

KEYWORDS: *difluoromethane, 1,1,1,2-tetrafluoroethane, 2,3,3,3-tetrafluoropropene, global warming, membrane separation, poly(ether-block-amide), R513A, R454B*

INTRODUCTION

Hydrofluorocarbons (HFCs), the 3rd generation of fluorinated gases (F-gases), are a family of synthetic compounds mainly used not only in the refrigeration and air conditioning (RAC) sector but also as aerosols and foam blowing agents because of their weak impact on depleting the stratospheric ozone, good thermodynamic performance, and negligible toxicity.[1] However, because of their very high global warming potential (GWP) and the sustained increase in HFC emissions since 1990, a roadmap has been established to gradually eliminate their production and use through several international agreements and regulations such as the Kigali Amendment to the Montreal Protocol and the European Regulation on F-gases.[2−6] Therefore, the current legislative and environmental framework demands the implementation of innovative technologies to improve the management of the end-of-life RAC equipment and promote the recovery, reuse, and recycling of refrigerants, with the aim of drastically reducing their emissions to the atmosphere.

In this context of transition to a low-carbon economy, some HFCs are being replaced by the 4th generation of F-gases, known as hydrofluoroolefins (HFOs), which present zero ozone depletion potential, negligible toxicity, reduced atmospheric lifetimes and thus GWPs that are several orders of magnitude below those of the most commonly used HFCs.[7] For instance, the HFO 2,3,3,3-tetrafluoropropene (R1234yf,

Received: January 29, 2021
Revised: April 29, 2021
Published: May 7, 2021

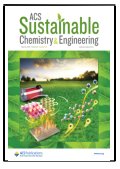

https://doi.org/10.1021/acssuschemeng.1c00668
ACS Sustainable Chem. Eng. 2021, 9, 7012–7021

GWP = 1) is replacing the HFC R134a (GWP = 1300) in automotive air conditioning. Therefore, a great variety of HFC/HFO mixtures with moderate GWP are currently being put on the RAC market as well. The most used HFCs in novel HFC/HFO mixtures are difluoromethane (R32, GWP = 677) and 1,1,1,2-tetrafluoroethane (R134a), whereas the most used HFOs are R1234yf and *trans*-1,3,3,3-tetrafluoropropene [R1234ze(E)], both with GWP = 1. Table 1 summarizes the

Table 1. Properties of Some HFC/HFO Refrigerant Mixtures Currently Used in the RAC Market[a]

HFC/HFO mixtures	HFC mol fraction	HFO mol fraction	temperature glide (K)	replacement for
R32 + R1234yf				
R454A (238)	0.54	0.46	5	R404A (3943)
R454B (467)	0.83	0.17	1.5	R410A (1924)
R454C (146)	0.38	0.62	6	R407C (1624), R404A (3943)
R134a + R1234yf				
R513A (573)	0.47	0.53	0 (azeotropic)	R134a (1300)
R513B (540)	0.44	0.56		

[a]The numbers in brackets present de GWP of each refrigerant blend as CO_2-eq.[14]

characteristics of some relevant HFC/HFO refrigerants obtained by blending these compounds (left-hand-side column) as well as some of the HFCs they are to replace (right-hand-side column). As can be seen, some of these HFC/HFO blends, such as those formed by the system R32/R1234yf, exhibit very low temperature difference between the saturated vapor temperature and the saturated liquid temperature (temperature glide). In addition, other mixtures are azeotropic and behave as a pure fluid, for example, blends of R134a and R1234yf.[8−11] Therefore, the separation of these mixtures into their constituents by conventional procedures such as cryogenic distillation is very challenging, if not impossible, in a cost-efficient way.[12,13]

Providing an effective response to address these challenging separations requires innovative approaches based on advanced separation processes. In this regard, notorious examples are the use of ionic liquids (ILs)[12,13,15−20] and deep eutectic solvents[21] as selective absorbents and entrainers in extractive distillation, as well as the use of activated carbons,[22,23] metal organic frameworks,[24] and zeolites[25] as selective adsorbents. Regarding the membrane technology, we assessed for the first time the gas permeation properties of HFC and HFO refrigerant gases through dense polymeric membranes made of poly(ether-*block*-amide), namely, Pebax grades 1657, 1074, and 2533.[26] In that work, we found that this family of copolymers enables the separation of HFCs from HFC/HFO mixtures, particularly through Pebax 1657, thanks to the low permeability of HFOs and high permeability of HFCs such as R32 and R134a. Moreover, we hypothesized that enhanced F-gas separation performances could be driven by the immobilization of selective ILs into the polymer matrix and demonstrated it for the separation of the constituents of the widely employed R410A blend, an equimass mixture of the HFCs R32 and R125, which is to be phased out.[27]

Therefore, in this work, we aim to extend our previous studies to the separation of a novel family of refrigerant blends containing HFOs, as the presence of these low-GWP fluorocarbons will be very significant in the RAC equipment over the next decades. Based on the promising results obtained through polymer membranes and considering that value-added HFCs such as R32 and R134a exhibit higher solubility in ILs than the HFO R1234yf, we expect these novel materials to improve the membrane separation performance in terms of permeability and selectivity. For this purpose, herein, we characterize the permeation properties and solubility of the F-gases R32, R134a, and R1234yf through composite IL−polymer membranes (CILPMs) prepared with the low-viscosity ILs $[C_2mim][SCN]$, $[C_2mim][BF_4]$, $[C_2mim][OTf]$, and $[C_2mim][Tf_2N]$. The influence of the IL anion moiety and content as well as the pressure effect on the transport properties and membrane stability is assessed. Eventually, the membranes with the best performance are evaluated for the separation of two commercial mixtures (R454B and R513A) under mixed-gas conditions to reveal their real separation potential for this application.

MATERIALS AND METHODS

Materials. The single F-gases R32 (99.9%), from Coproven Climatización (Gas Servei licensed supplier), R134a (99.8%), and R1234yf (99.9%), from Carburos Metálicos (Air Products Group), were used in the single gas permeation and sorption tests. The HFC/HFO refrigerant blends R513A and R454B (Coproven Climatización) were used in the mixed gas permeation tests. Table S1 of the Supporting Information summarizes the main properties of the F-gases used in this work.

The polymer used to fabricate dense membranes was poly(ether-*block*-amide) (Pebax 1657MH grade), which was kindly provided as pellets by Arkema Química SAU (Spain). The Pebax 1657MH grade consists of rigid segments of polyamide 6 (40 wt %) and flexible units of polyethylene oxide (PEO) (60 wt %). On the other hand, the polyamide segments (melting temperature = 215 °C) give to this family of copolymers good mechanical resistance, whereas the PEO units (melting temperature = 67 °C) provide elasticity and facilitate the transport of gas penetrants through the polymer film. Butan-1-ol (99.9%), from VWR, was employed as the solvent for the polymer and polymer−IL mixtures.

The IL 1-ethyl-3-methylimidazolium thiocyanate, $[C_2mim][SCN]$ (>98%), was purchased from IoLiTec, whereas 1-ethyl-3-methylimidazolium tetrafluoroborate, $[C_2mim][BF_4]$ (>98%), 1-ethyl-3-methylimidazolium trifluoromethanesulfonate, $[C_2mim][OTf]$ (>98%), and 1-ethyl-3-methylimidazolium bis[(trifluoromethyl)-sulfonyl]imide, $[C_2mim][Tf_2N]$ (>98%), were purchased from Sigma-Aldrich. The selected ILs are categorized as low-viscosity ILs, which added to their virtually no volatility, and good compatibility with the polymer Pebax 1657 makes them excellent candidates for the fabrication of composite membranes.[11,27] Table S2 of the Supporting Information shows general properties of the ILs used in this work.

Membrane Preparation. Pure polymer membranes and CILPMs were manufactured by the solvent casting method using butanol as a solvent to avoid risks of hydrolysis of the fluorinated ILs.[28,29] 3 wt % of polymer was dissolved in butan-1-ol at 100 °C under magnetic agitation. Once the polymer was dissolved, the corresponding amount of IL was added, and agitation was maintained at 100 °C for 1 h to ensure correct homogenization and to avoid premature gelation of the polymer−IL solution. Subsequently, the solution was poured onto a glass Petri dish, and the solvent was evaporated in a vacuum oven at 300 mbar absolute pressure and 40 °C. The thickness of the membranes was measured with a Mitutoyo digital micrometer (MDC-25PX, accuracy ±1 μm), obtaining the average thickness from nine measurements at different points of the dense film. The average thickness measured for all the membranes tested was 100 ± 10 μm. In total, 11 stable and mechanically suitable membranes were manufactured with IL compositions ranging from 20 to 60 wt %.

https://doi.org/10.1021/acssuschemeng.1c00668
ACS Sustainable Chem. Eng. 2021, 9, 7012−7021

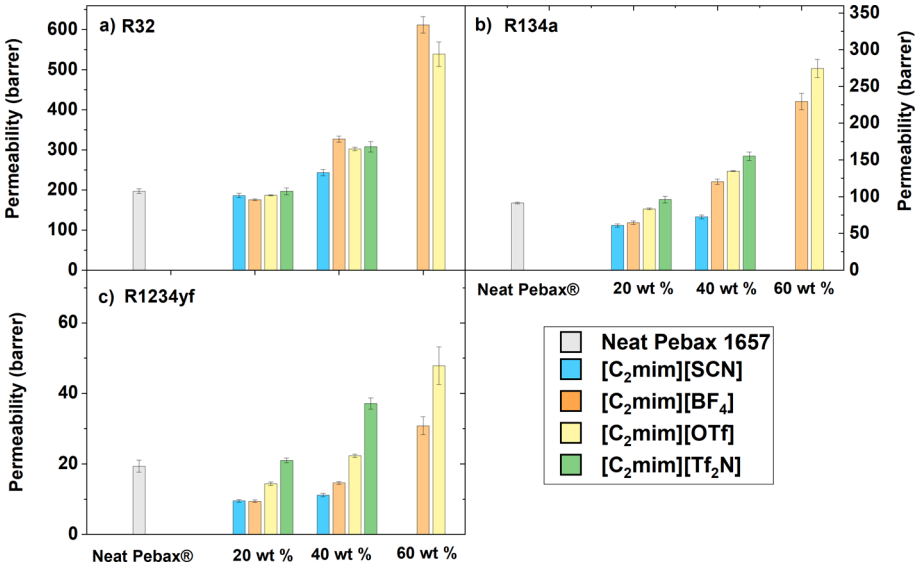

Figure 1. Single gas permeability of R32 (a), R134a (b), and R1234yf (c) through neat Pebax 1657 and several CILPMs as a function of the IL content (in the *X*-axis) and the anion type (color code in the legend). Data were obtained at 1.3 bar feed pressure and 30 °C.

Gas Permeability Measurements. The gas permeability through polymer and CILPMs is described according to the solution-diffusion model (eq 1)

$$P = D \cdot S \tag{1}$$

where P, D, and S are the permeability, diffusion, and solubility coefficients, respectively. The single gas permeability tests were performed using an experimental apparatus working in a steady state, as described in our previous works.[30−32] In summary, pure F-gas (R32, R134a, or R1234yf) or the HFC/HFO commercial blend (R513A and R454B) enters the retentate side of the membrane allocated inside a custom-made stainless-steel cell. The pressure in the retentate side is controlled by a back-pressure regulator installed at the outlet port of the retentate stream. In the permeate side, an argon stream is used as sweep gas. For the pure F-gases and the mixture R454B, the permeate stream is analyzed with a micro-gas chromatograph (Agilent 490) equipped with a PoraPLOT U column and a thermal conductivity detector. In the case of the R513A mixture, the permeate gas was analyzed in a gas chromatograph coupled to a mass spectrometry detector (Shimadzu QP2010), equipped with a GasPro column, which allowed the adequate separation of the chromatographic peaks of R134a and R1234yf. The gas permeability coefficient is calculated according to eq 2

$$P_i = \frac{Q_i \cdot \delta}{A \cdot (f_{R,i} - f_{p,i})} \tag{2}$$

where P_i is the permeability coefficient, Q_i is the transmembrane flow of component i through the membrane, δ is the membrane thickness, A is the membrane permeation area, and $f_{R,i}$ and $f_{p,i}$ are the fugacity of component i in the retentate and permeate, respectively. Accordingly, fugacity is calculated using eq 3

$$f_i = \emptyset_i \cdot p_i \tag{3}$$

where $\emptyset_i$ and p_i are the fugacity coefficient and partial pressure of component i, respectively. $\emptyset_i$ is obtained from the property method REFPROP (NIST Reference Fluid Thermodynamic and Transport Properties Database), enabled in Aspen Plus V10 through the property analysis tool; this method uses explicit Helmholtz energy equations of state optimized for the refrigerants of this study, namely, R32,[33] R134a,[34] and R1234yf.[35] In the case of R513A and R454B, the corresponding mixed-gas fugacity of each compound in the mixture is employed.

Finally, the ideal HFC/HFO permselectivity ($\alpha_{HFC/HFO}$) is calculated as the ratio between the HFC (P_{HFC}) and HFO (P_{HFO}) permeability coefficients (eq 4)

$$\alpha_{HFC/HFO} = \frac{P_{HFC}}{P_{HFO}} \tag{4}$$

Gas Sorption Measurements. The experimental apparatus for the determination of the solubility coefficient (S) of the F-gases in polymer and composite membranes is based on the pressure decay method (Figure S1 of the Supporting Information).[36−38] It consists of a sorption chamber (22 mL capacity stainless-steel Parr reactor) connected to a reservoir (50 mL stainless-steel cylinder) by a valve. The total volume of the sorption system including tubing elements is 93 mL. To guarantee isothermal operation in the sorption experiments, the system is immersed in a thermostatized bath (Grant Optima TX150 heated circulating bath, temperature uniformity ±0.05 °C). Pressure and temperature measurements in both the sorption chamber and the reservoir are monitored and registered online over time with absolute pressure sensors (Keller PAA-33X series, 0.02% accuracy at a full scale).

A sample of the dense film membrane (~3 g) is placed inside the sorption chamber, rolled up and sandwiched between stainless-steel mesh spacers. Prior to each sorption test, the dense film is subjected to desorption under high vacuum and 30 °C for 24 h to eliminate solvent and moisture residues. In each test, the gas (R32, R34a, or R1234yf) is loaded into the reservoir at the desired pressure. Meanwhile, the sorption chamber remains at near-vacuum absolute pressure (<0.5 mbar). Once pressure and temperature are stabilized in the reservoir, the valve connecting both sections is opened and the sorption process occurs spontaneously until equilibrium is reached (no pressure changes for 30 min). To obtain a complete sorption isotherm, the process is repeated by loading the reservoir at a higher pressure in each stage. The ratio between the total volume of the sorption setup and the sample volume introduced is above 30:1, which minimizes the effect of film expansion by the sorbed gas in the determination of the sorption isotherms.

Therefore, the amount of gas absorbed in each equilibrium step ($n_{i,j}$) is calculated as the difference between the amount of gas initially loaded in the reservoir and the remaining gas (not absorbed) after reaching equilibrium conditions according to eq 5

$$n_{i,j} = \rho_{(i,j,R)} \cdot V_R + \rho_{(i,j-1,S)} \cdot (V_S - V_F - V_M) - \rho_{(i,j,S)} \cdot (V_R + V_S - V_F - V_M) \tag{5}$$

https://doi.org/10.1021/acssuschemeng.1c00668
ACS Sustainable Chem. Eng. 2021, 9, 7012−7021

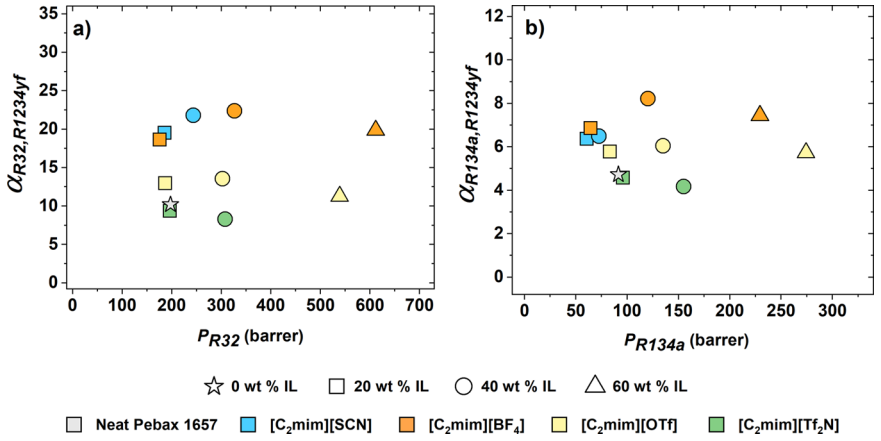

Figure 2. Ideal HFC/HFO permselectivity as a function of the IL content and anion type with respect to HFC permeability for the system R32 + R1234yf (a) and R134a + R1234yf (b). Data were obtained at 1.3 bar feed pressure and 30 °C.

where $\rho_{(i,j,R)}$, $\rho_{(i,j-1,S)}$, and $\rho_{(i,j,S)}$ are the molar densities (mol·L^{-1}) of gas i in the reservoir, in the sorption chamber at the previous equilibrium conditions, and in the total available volume after reaching the new equilibrium conditions, respectively. V_R, V_S, V_F, and V_M are the volumes of reservoir, sorption chamber, dense film, and stainless-steel mesh spacers, respectively. F-gas molar densities were calculated from the experimental data (pressure and temperature) using the property analysis tool of Aspen Plus V10 with the REFPROP property method.

The total amount of gas i sorbed in the polymer in each step ($n_{i,\text{total}}$) is then calculated as the moles sorbed in the last step $n_{i,j}$ plus the accumulated moles sorbed in the previous k steps (eq 6)

$$n_{i,\text{total}} = n_{i,j} + \sum_{k=1}^{j-1} n_{i,k} \tag{6}$$

Finally, the gas concentration at each equilibrium step [$C_{i,\text{eq}}$, cm^3(STP)$_{\text{gas}}$·cm$_{\text{film}}^{-3}$] is calculated from the total moles sorbed $n_{i,\text{total}}$, film volume V_F, and the molar volume of an ideal gas under standard pressure and temperature conditions [22,414 cm^3(STP) mol^{-1}] as follows

$$C_{i,\text{eq}} = \frac{22{,}414 \cdot n_{i,\text{total}}}{V_F} \tag{7}$$

RESULTS AND DISCUSSION

Screening of the CILPM Separation Potential. Figure 1 shows the single gas permeability through the neat polymer membrane and several CILPMs as a function of the IL content at 1.3 bar of feed pressure and 30 °C. The ILs considered for the comparison are [C_2mim][SCN], [C_2mim][BF_4], [C_2mim][OTf], and [C_2mim][Tf_2N], and the IL concentration is studied in the range of 20−60 wt %. It is worth mentioning that composite membranes with 60 wt % of [C_2mim][SCN] and [C_2mim][Tf_2N] did not present the mechanical properties required to perform any gas permeation test because of their fragility, thus results concerning these films are not shown in Figure 1.

First, a well-reported trend is observed; the permeability of all studied gases through CILPMs increases at higher IL concentrations as a result of increased polymer chain mobility within the composite film.[39−41] It is also verified that the order of gas permeability, that is, R32 > R134a > R1234yf, is consistent with the lower molecular size of R32 compared to that of R134a and R1234yf, as already stated in our previous work[26] regarding the permeation properties of these gases through polymer membranes prepared with different Pebax grades.

With respect to the anion of the ILs used, the permeability of R32, R134a, and R1234yf through CILPMs increases following the same order as the IL molar volume, SCN < BF_4 < OTf < Tf_2N, except for the permeability of R32 in [C_2mim][BF_4] that is slightly higher than through the other ILs. This trend is ascribed to the fact that ILs with a higher degree of fluorination and larger molecular size exhibit higher solubility values toward F-gases.[16,17,42,43] Accordingly, the solubility of the F-gas in the IL in the question plays a key role in the permeation of F-gases through this type of CILPMs, since in turn, according to the solution-diffusion model (eq 1), permeability depends largely on the solubility of the penetrant in the dense film. The highest permeability values are given in the membranes with 60 wt % IL. For R32, which is the smallest gas, the membrane with 60 wt % of [C_2mim][BF_4] presents a permeability 3 times higher (612 barrer) than that in the pure polymer (197 barrer). For larger gases, that is, R134a and R1234yf, the greatest promotion of permeability is given by the membrane with 60 wt % of [C_2mim][OTf], which compared to the neat polymer increased R134a permeability from 92 to 274 barrer and R1234yf permeability from 19 to 48 barrer.

Furthermore, it is observed that the Pebax-based IL composite membranes may perform efficiently for the separation of HFCs from HFOs for two of the most relevant systems found in novel low-GWP HFC/HFO refrigerant blends, that is, R32/R1234yf and R134a/R1234yf (see Table 1). Figure 2a presents the ideal permeability selectivity for the R32/R1234yf system as a function of the IL content and anion type with respect to the HFC permeability. As can be seen, the membranes containing [C_2mim][SCN] and [C_2mim][BF_4] greatly improve the permselectivity, by more than 100%, with respect to the pure polymer. Specifically, excellent selectivity values are obtained for the separation of the gas pair R32/R1234yf by the membrane with 40 wt % [C_2mim][SCN], $\alpha_{\text{R32/R1234yf}}$ = 21.8 and by the membranes with 40 and 60 wt % [C_2mim][BF_4], $\alpha_{\text{R32/R1234yf}}$ = 22.4 and 19.8, respectively. Very interestingly, one of the main reasons of such improvements is the marked reduction of R1234yf permeability, which decreases from 19.4 barrer in the pure polymer to 11.2 barrer in the membrane with 40 wt % [C_2mim][SCN] and to 14.6 barrer in the membrane with 40 wt % [C_2mim][BF_4]. In contrast, for the CILPMs containing bigger anions, that is,

https://doi.org/10.1021/acssuschemeng.1c00668
ACS Sustainable Chem. Eng. 2021, 9, 7012−7021

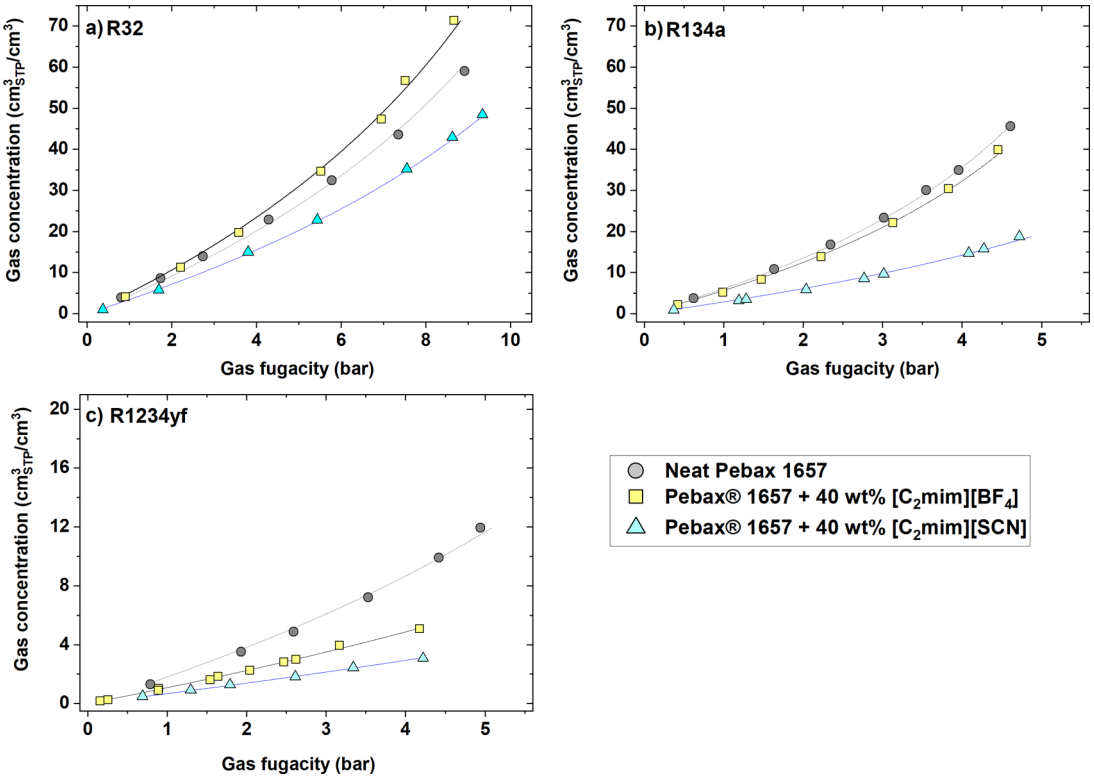

Figure 3. Membrane gas sorption equilibrium data. F-gas concentration [(a) R32, (b) R134a, and (c) R1234yf] sorbed in the membrane phase as a function of solute fugacity in the gas phase. Solid lines correspond to the fit of experimental data to the Flory–Huggins model (eq 8) with the parameters listed in Table 2.

[C_2mim][OTf] and [C_2mim][Tf_2N], the separation performance is not significantly enhanced with respect to that observed for the pure polymer or even decreases in the case of [C_2mim][Tf_2N]–CILPMs ($\alpha_{R32/R1234yf}$ = 8.3 at 40 wt % IL).

For the separation of R134a/R1234yf mixtures (Figure 2b), the CILPMs exhibit a somewhat lower separation potential than the R32/R1234yf pair, which may be attributed to a much narrower molecular size difference between R134a and R1234yf (see the Chung diameter in Table S1). Nonetheless, the ideal selectivity of neat Pebax 1657 ($\alpha_{R134a,R1234yf}$ = 4.7) is also significantly enhanced using CILPMs. The permselectivity increases up to 6.5 in the membrane with 40 wt % [C_2mim][SCN] and 8.2 in the membrane with 40 wt % [C_2mim][BF_4]. Conversely, the selectivity is just slightly higher than that of the pure polymer in the 40 wt % [C_2mim][OTf]–CILPM and much lower in the 40 wt % [C_2mim][Tf_2N]–CILPM. In a similar way to R32/R1234yf separation, the largest anions with a significant degree of fluorination, such as OTf and Tf_2N, exhibit lower separation capacity toward the R134a/R1234yf pair, which is consistent with the reported low solubility selectivity in ILs for this pair of gases.[11] Overall, these results suggest that although F-gas permeability through ILs is favored by strong enthalpic interactions (F-gases exhibit large electric dipole moments and H-bonding capability), the HFC/HFO separation selectivity may benefit from unfavorable entropic effects that hinder the solvation of large solutes in low-molar volume ILs, a fact that is in good agreement with available F-gas solubility studies in ILs.[11,16]

F-Gas Sorption Behavior in Pebax 1657 CILPMs. Understanding the effect of pressure on the membrane gas solubility is a critical aspect for designing membrane-based separation processes, particularly regarding the permeation of highly soluble penetrants such as CO_2, organic vapors, and fluorinated hydrocarbon gases, whose transport properties through rubbery polymers strongly depend on pressure.[44−47] Thus, we have studied the sorption behavior of R32, R134a, and R1234yf as a function of pressure in CILPMs. For this study, we selected the CILPM materials with the best performance in terms of R32/R1234yf and R134a/R1234yf permselectivity and stability toward feed pressure, that is, the CILPMs with 40 wt % [C_2mim][SCN] and [C_2mim][BF_4], as well as the neat polymer Pebax 1657, for the sake of comparison. Eventually, CILPMs with 60 wt % IL were not considered, as they became mechanically unstable when tested in the permeation cell at feed pressures above 4 bar.

The results plotted in Figure 3 show the gas concentration absorbed in the neat polymer film and CILPMs as a function of the fugacity of R32 (3a), R134a (3b), and R1234yf (3c). On the other hand, the immobilization of 40 wt % [C_2mim][SCN] within the polymer matrix causes a significant decrease in the sorption capacity of all gases with respect to that of the pure Pebax 1657, which confirms the hypothesis of the solubility blockage phenomenon previously stated. In contrast, the influence of incorporating [C_2mim][BF_4] to the CILPM material is different for each gas. The solubility of R32 improves with respect to that of the pure polymer, while the solubility of R134a remains practically unchanged and that of R1234yf is reduced, yet not as much as with [C_2mim][SCN].

As can be seen, the convex shape to the fugacity axis of all isotherms suggests that the gas sorption behavior in this type of IL composite membrane materials can be described using the Flory–Huggins regular solution model (eq 8) commonly applied to the nonspecific sorption of gases in rubbery

https://doi.org/10.1021/acssuschemeng.1c00668
ACS Sustainable Chem. Eng. 2021, 9, 7012−7021

Table 2. Fitted Flory–Huggins Interaction Parameter (χ) of R32, R134a, and R1234yf in Pebax 1657-Based CILPMs[a]

penetrant	neat Pebax 1657	Pebax 1657 + 40 wt % [C_2mim][SCN]	Pebax 1657 + 40 wt % [C_2mim][BF_4]
R32	0.85	1.08	0.71
R134a	0.95	1.68	1.03
R1234yf	1.92	2.88	2.42

[a]Experimental standard deviation < 5%.

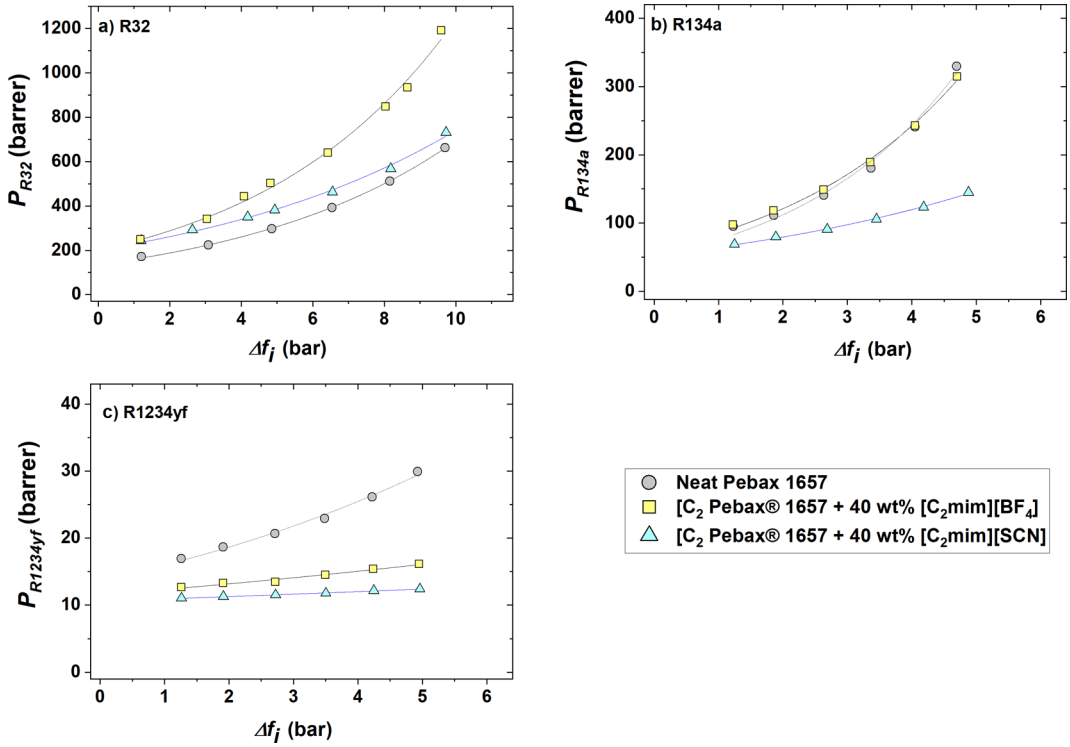

Figure 4. Pressure influence on single gas permeability as a function of transmembrane fugacity through CILPMs at 30 °C.

polymers.[48] This model provides an accurate description of the sorption behavior of condensable gases and vapors that lead to solute cluster formation with increasing activity.[49] In this regard, several works have previously reported the adequacy of using the Flory–Huggins model to fit convex-shaped sorption isotherms[50] of different solvent vapors, such as methanol, ethanol, or butanol, in membranes made of the family of Pebax copolymers[51] or the sorption of water vapor through the Pebax 1074 grade.[52] Besides, good correlations were found for the sorption of CO_2 in similar polymers to Pebax, such as crosslinked PEO[38] or crosslinked PEO diacrylate membranes.[53] However, to the best of our knowledge, this model has not been widely applied to describe gas solubility in CILPMs.

$$\ln \frac{f}{f_{sat}} = \ln \upsilon_i + (1 - \upsilon_i) + \chi(1 - \upsilon_i)^2 \quad (8)$$

In eq 8, f and f_{sat} are the gas fugacity and saturation fugacity at the corresponding equilibrium pressure and temperature, respectively, υ_i is the volume fraction of the penetrant dissolved in the polymer, and χ is the Flory–Huggins interaction parameter. In addition, eq 9 allows calculating υ_i from the equilibrium gas concentration (eq 7) and the F-gas liquid molar volume $\overline{V}$ ($cm^3\ mol^{-1}$), obtained with the REFPROP property method, at the sorption equilibrium temperature[38]

$$\upsilon_i = \frac{C_{i,eq}\overline{V}}{22{,}414 + C_{i,eq}\overline{V}} \quad (9)$$

Table 2 summarizes the Flory–Huggins interaction parameter (χ) obtained for each F-gas/membrane pair after fitting of experimental data to eqs 8 and 9. The results shown in Figure 3, in which the solid lines present the simulated values, indicate that the Flory–Huggins model shows very good accuracy ($r^2 > 0.996$) for the description of the HFC and HFO sorption behavior over a wide pressure range (1–10 bar for R32 and 1–5.5 bar for R134a and R1234yf) in both the neat polymer and the CILPMs. According to the model, the penetrant–polymer interactions become less important as χ parameter increases, particularly the polymer–gas interactions are small when $\chi > 2$ and very strong when $\chi < 0.5$.[49] Therefore, the calculated χ parameter is in very good agreement with the experimental solubility behavior observed in Figure 3; the solute–neat polymer interactions are significant for R32 and R134a and much less important for R1234yf. However, after [C_2mim][SCN] and [C_2mim][BF_4] immobilization, the solute–CILPM interactions become weaker (i.e., the value of χ increases), except for the system R32–40 wt % [C_2mim][BF_4]–CILPM, for which the gas–CILPM interactions are stronger (i.e., the value of χ decreases).

Pressure Effect on CILPM Permeability. To further understand the influence of IL presence on F-gas permeability,

https://doi.org/10.1021/acssuschemeng.1c00668
ACS Sustainable Chem. Eng. 2021, 9, 7012–7021

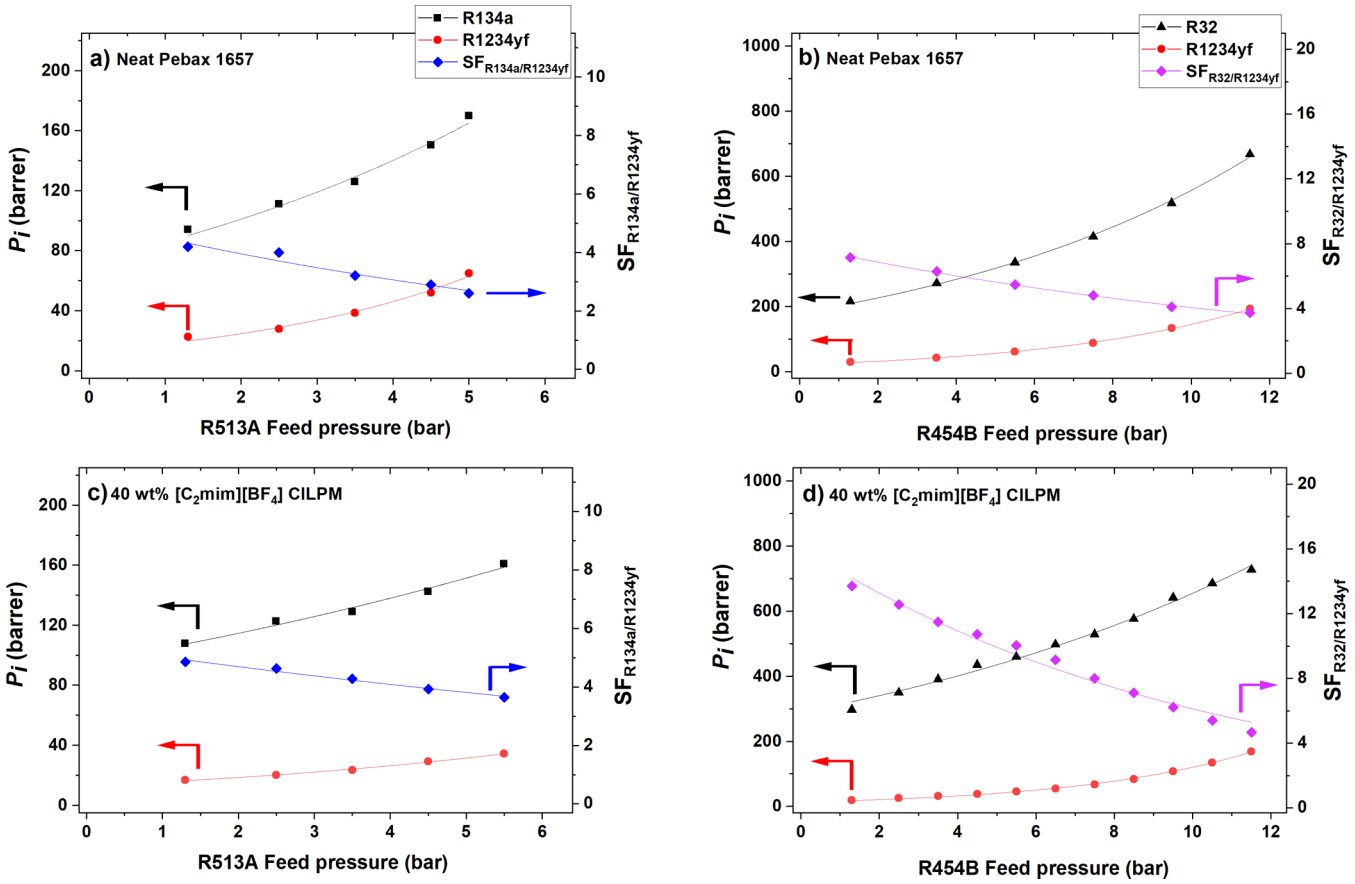

Figure 5. Gas permeability (left axis) and SF (right axis) as a function of feed pressure for R513A (a,c) and R454B (b,d) refrigerant mixtures through neat Pebax 1657 (a,b) and 40 wt % [C_2mim][BF_4]−CILPM (c,d).

we have studied the effect of pressure on single gas permeability of R32, R134a, and R1234yf. In this regard, Figure 4 shows the single F-gas permeability as a function of transmembrane fugacity through the same dense films selected for the solubility study, that is, neat Pebax 1657, Pebax 1657−40 wt % [C_2mim][SCN], and Pebax 1657−40 wt % [C_2mim][BF_4]. As expected for this sort of materials, the permeability of highly condensable refrigerant gases exponentially increases with pressure according to eq 10.[26,27,54]

$$P = P_0 \cdot e^{m \cdot \Delta f} \tag{10}$$

where P_0 is the preexponential parameter corresponding to the gas permeability through the dense film at infinite dilution, m is the coefficient that provides information about the effect of pressure on permeability, and Δf is the transmembrane fugacity between the retentate and permeate sides of the membrane. The parameters obtained by fitting the experimental data to eq 10 are summarized in Table S3 of the Supporting Information.

Interestingly, the permeability profiles of the two largest molecules studied, R134a (Figure 4b) and R1234yf (Figure 4c), exhibit the same trends observed for the sorption isotherms, that is, the presence of [C_2mim][SCN] and [C_2mim][BF_4] leads to lower solubility and permeability values compared to the neat polymer, thus revealing a predominant solubility control of the separation properties in these CILPMs. In contrast, for the fastest and smallest molecule, R32 (Figure 4a), the presence of both ILs in the membrane markedly enhances permeability at increasing pressure, particularly for the [C_2mim][BF_4]−CILPM. This effect is attributed to an improved diffusivity of R32 through the CILPM over that of the neat polymer, given that the addition of [C_2mim][BF_4] only slightly improves R32 solubility and the addition of [C_2mim][SCN] worsens R32 solubility, as previously shown in Figure 3a.

Separation Performance of Real HFC/HFO Mixtures. While the results outlined in the previous sections, obtained from pure gas permeation and sorption experiments, are of high value to discriminate between different materials and to understand the individual behavior of each gas, mixed-gas permeation tests provide critical information in terms of the potential applicability of this separation technology to real case studies. Therefore, in this work, we have studied the separation performance of the 40 wt % [C_2mim][BF_4]−CILPM membrane, which provided the best results in terms of permeability and R32/R1234yf and R134a/R1234yf gas pair ideal selectivity, toward the separation of two relevant commercial HFC/HFO mixtures, namely, R513A (47 mol % R134a and 53 mol % R1234yf) and R454B (83 mol % R32 and 17 mol % R1234yf). In this regard, Figure 5 shows the permeability of each component of the mixtures R513A (Figure 5a,c) and R454B (Figure 5b,d) and the separation factor (SF), which is defined by eq 11, as a function of the mixture feed pressure through neat Pebax 1657 and the 40 wt % [C_2mim][BF_4]−CILPM.

$$SF = \frac{x^{p}_{HFC}/x^{p}_{HFO}}{x^{f}_{HFC}/x^{f}_{jHFO}} \tag{11}$$

https://doi.org/10.1021/acssuschemeng.1c00668
ACS Sustainable Chem. Eng. 2021, 9, 7012−7021

where x_{HFC} and x_{HFO} are the mole fractions of HFC and HFO and the superscripts p and f stand for the permeate and feed side of the membrane, respectively.

The results confirm that the 40 wt % $[C_2mim][BF_4]$−CILPM exhibits higher separation performance than the pure polymer for both R32/R1234yf and R134a/R1234yf gas pairs. Besides, the SF for R32/R1234yf is higher than that for R134a/R1234yf in both membranes. In any case, the permeability of each constituent in the mixture increases exponentially with feed pressure, but the SF decreases progressively from 4.9 at 1.3 bar to 3.6 at 5.5 bar for the separation of R513A compounds in the CILPM and from 4.2 at 1.3 bar to 2.6 at 5 bar in the neat Pebax film. On the other hand, for R454B species, the SF decreases from 13.7 at 1.3 bar to 4.7 at 11.5 bar in the CILPM, whereas in the neat polymer, the decrease is from 7.1 at 1.3 bar to 3.7 at 11.5 bar. This decrease is attributed to the plasticization effect of high-sorbing HFC penetrants, which leads to a sharper increase with pressure of the R1234yf permeability compared to that observed with the pure gas. In fact, this behavior is expected in rubbery polymer and rubbery polymer-based composite materials.[27]

At this point, the SF experimentally achieved for the separation of the R513A mixture with the 40 wt % $[C_2mim][BF_4]$−CILPM can be compared to that predicted by Albà et al.[19] for an extractive distillation process that uses $[C_6mim][BF_6]$ as an entrainer, 3.65 at 298 K, which is in the lower limit of the SFs achieved in this work working with real mixtures and the membrane technology.

CONCLUSIONS

The purpose of this work is framed within the needs of avoiding high-GWP gas emissions and developing novel separation technologies to boost recycling strategies and improve resource use in the race toward zero-emissions in the RAC sector. The emphasis is set on the separation of a novel class of refrigerant blends constituted by an HFC (R32 or R134a) and the HFO R1234yf through polymer membranes functionalized with several ILs. Results show that carefully engineered CILPMs improve the separation of HFC/HFO mixtures in terms of gas permeability and selectivity. The CILPMs exhibiting the best performance and mechanical stability were those prepared with 40 wt % $[C_2mim][SCN]$ and $[C_2mim][BF_4]$. Their performance to separate commercial refrigerants (R454B and R513A) was tested at relevant pressures relative to the mixture vapor pressure (up to 12 bar). These CILPMs show high HFC permeability and HFC/HFO selectivity, yet the SF decreases as the feed pressure increases. Accordingly, the use of advanced materials in membrane separation processes can be sought as a promising strategy to enable the separation of azeotropic and close-boiling-point HFC/HFO mixtures.

ASSOCIATED CONTENT

Supporting Information

The Supporting Information is available free of charge at https://pubs.acs.org/doi/10.1021/acssuschemeng.1c00668.

Physical properties of refrigerants R32, R134a, and R1234yf used in this work and their mixtures; properties of the ILs used in this work at 30 °C and 1 bar; parameters of the exponential fitting to eq 10, and schematic diagram of the dual-volume pressure decay sorption system (PDF)

AUTHOR INFORMATION

Corresponding Author

Ane Urtiaga − *Department of Chemical and Biomolecular Engineering, Universidad de Cantabria, Santander 39005, Spain;* orcid.org/0000-0002-8189-9171; Email: urtiaga@unican.es

Authors

Fernando Pardo − *Department of Chemical and Biomolecular Engineering, Universidad de Cantabria, Santander 39005, Spain;* orcid.org/0000-0001-9821-0310

Sergio V. Gutiérrez-Hernández − *Department of Chemical and Biomolecular Engineering, Universidad de Cantabria, Santander 39005, Spain*

Gabriel Zarca − *Department of Chemical and Biomolecular Engineering, Universidad de Cantabria, Santander 39005, Spain;* orcid.org/0000-0002-4072-4252

Complete contact information is available at: https://pubs.acs.org/10.1021/acssuschemeng.1c00668

Notes

The authors declare no competing financial interest.

ACKNOWLEDGMENTS

Authors fully acknowledge the financial support received from Project KET4F-Gas-SOE2/P1/P0823, which is cofinanced by the European Regional Development Fund within the framework of Interreg Sudoe Programme, and project PID2019-105827RB-I00—Agencia Estatal de Investigación, Spain. F.P. acknowledges the postdoctoral fellowship (FJCI-2017-32884 Juan de la Cierva Formación) awarded by the Spanish Ministry of Science, Innovation and Universities.

REFERENCES

(1) Sicard, A. J.; Baker, R. T. Fluorocarbon Refrigerants and their Syntheses: Past to Present. *Chem. Rev.* **2020**, *120*, 9164−9303.

(2) McLinden, M. O.; Huber, M. L. (R)Evolution of Refrigerants. *J. Chem. Eng. Data* **2020**, *65*, 4176−4193.

(3) United Nations Environment Programme. Decision XXVIII/-Further Amendment of the Montreal Protocol. *Twenty-Eighth Meeting of the Parties to the Montreal Protocol on Substances that Deplete the Ozone Layer*, Kigali, Oct 10−14, 2016. https://ozone.unep.org/treaties/montreal-protocol/meetings/twenty-eighth-meeting-parties/decisions/annex-i-amendment (accessed May 6, 2021).

(4) The European Parliament and the Council of the European Union. Regulation (EU) No 517/2014 of the European Parliament and the Council of 16 April 2014 on fluorinated greenhouse gases and repealing Regulation (EC) No 842/2006. *Official Journal of the European Union*, 2014; Vol. *150*, pp 195−230. https://eur-lex.europa.eu/legal-content/EN/TXT/?uri=celex%3A32014R0517 (accessed May 6, 2021).

(5) Senators strike deal for US phasedown of HFCs. *C&EN Global Enterprise*, 2020; Vol. *98*, 36, p 16.

(6) 116th Congress 1st Session. Sen. Kennedy, John [R-LA] (Introduced 10/30/2019). In The Senate of The United States. Bill S.2754—American Innovation and Manufacturing Act of 2019. https://www.congress.gov/bill/116th-congress/senate-bill/2754/text (accessed May 6, 2021).

(7) Minor, B. H.; Herrmann, D.; Gravell, R. Flammability characteristics of HFO-1234yf. *Process Saf. Prog.* **2010**, *29*, 150−154.

(8) Makhnatch, P.; Mota-Babiloni, A.; López-Belchí, A.; Khodabandeh, R. R450A and R513A as lower GWP mixtures for

high ambient temperature countries: Experimental comparison with R134a. *Energy* **2019**, *166*, 223−235.
(9) Bobbo, S.; Fedele, L.; Curcio, M.; Bet, A.; De Carli, M.; Emmi, G.; Poletto, F.; Tarabotti, A.; Mendrinos, D.; Mezzasalma, G.; Bernardi, A. Energetic and exergetic analysis of low global warming potential refrigerants as substitutes for R410A in ground source heat pumps. *Energies* **2019**, *12*, 3538.
(10) Heredia-Aricapa, Y.; Belman-Flores, J. M.; Mota-Babiloni, A.; Serrano-Arellano, J.; García-Pabón, J. J. Overview of low GWP mixtures for the replacement of HFC refrigerants: R134a, R404A and R410A. *Int. J. Refrig.* **2020**, *111*, 113−123.
(11) Asensio-Delgado, S.; Pardo, F.; Zarca, G.; Urtiaga, A. Vapor−Liquid Equilibria and Diffusion Coefficients of Difluoromethane, 1,1,1,2-Tetrafluoroethane, and 2,3,3,3-Tetrafluoropropene in Low-Viscosity Ionic Liquids. *J. Chem. Eng. Data* **2020**, *65*, 4242−4251.
(12) Asensio-Delgado, S.; Pardo, F.; Zarca, G.; Urtiaga, A. Enhanced absorption separation of hydrofluorocarbon/hydrofluoroolefin refrigerant blends using ionic liquids. *Sep. Purif. Technol.* **2020**, *249*, 117136.
(13) Shiflett, M. B.; Yokozeki, A. Separation of difluoromethane and pentafluoroethane by extractive distillation using ionic liquid. *Chim. Oggi* **2006**, *24*, 28−30.
(14) IPCC. Summary for Policymakers. In *Climate Change 2013: The Physical Science Basis. Contribution of Working Group I to the Fifth Assessment Report of the Intergovernmental Panel on Climate Change*; Stocker, T. F., Qin, D., Plattner, G.-K., Tignor, M., Allen, S. K., Boschung, J., Nauels, A., Xia, Y., Bex, V., Midgley, P. M., Eds.; Cambridge University Press: Cambridge, United Kingdom and New York, NY, USA, 2013.
(15) Asensio-Delgado, S.; Jovell, D.; Zarca, G.; Urtiaga, A.; Llovell, F. Thermodynamic and process modeling of the recovery of R410A compounds with ionic liquids. *Int. J. Refrig.* **2020**, *118*, 365−375.
(16) Lepre, L. F.; Andre, D.; Denis-Quanquin, S.; Gautier, A.; Pádua, A. A. H.; Costa Gomes, M. Ionic Liquids Can Enable the Recycling of Fluorinated Greenhouse Gases. *ACS Sustainable Chem. Eng.* **2019**, *7*, 16900−16906.
(17) Sosa, J. E.; Ribeiro, R. P. P. L.; Castro, P. J.; Mota, J. P. B.; Araújo, J. M. M.; Pereiro, A. B. Absorption of Fluorinated Greenhouse Gases Using Fluorinated Ionic Liquids. *Ind. Eng. Chem. Res.* **2019**, *58*, 20769−20778.
(18) Sosa, J. E.; Santiago, R.; Hospital-Benito, D.; Costa Gomes, M.; Araújo, J. M. M.; Pereiro, A. B.; Palomar, J. Process Evaluation of Fluorinated Ionic Liquids as F-Gas Absorbents. *Environ. Sci. Technol.* **2020**, *54*, 12784−12794.
(19) Albà, C. G.; Vega, L. F.; Llovell, F. Assessment on Separating Hydrofluoroolefins from Hydrofluorocarbons at the Azeotropic Mixture R513A by Using Fluorinated Ionic Liquids: A Soft-SAFT Study. *Ind. Eng. Chem. Res.* **2020**, *59*, 13315−13324.
(20) Morais, A. R. C.; Harders, A. N.; Baca, K. R.; Olsen, G. M.; Befort, B. J.; Dowling, A. W.; Maginn, E. J.; Shiflett, M. B. Phase Equilibria, Diffusivities, and Equation of State Modeling of HFC-32 and HFC-125 in Imidazolium-Based Ionic Liquids for the Separation of R-410A. *Ind. Eng. Chem. Res.* **2020**, *59*, 18222−18235.
(21) Castro, P. J.; Redondo, A. E.; Sosa, J. E.; Zakrzewska, M. E.; Nunes, A. V. M.; Araújo, J. M. M.; Pereiro, A. B. Absorption of Fluorinated Greenhouse Gases in Deep Eutectic Solvents. *Ind. Eng. Chem. Res.* **2020**, *59*, 13246−13259.
(22) El-sharkawy, M. M.; Askalany, A. A.; Harby, K.; Ahmed, M. S. Adsorption isotherms and kinetics of a mixture of Pentafluoroethane, 1,1,1,2-Tetrafluoroethane and Difluoromethane (HFC-407C) onto granular activated carbon. *Appl. Therm. Eng.* **2016**, *93*, 988−994.
(23) Sosa, J. E.; Malheiro, C.; Ribeiro, R. P.; Castro, P. J.; Piñeiro, M. M.; Araújo, J. M.; Plantier, F.; Mota, J. P.; Pereiro, A. B. Adsorption of fluorinated greenhouse gases on activated carbons: evaluation of their potential for gas separation. *J. Chem. Technol. Biotechnol.* **2020**, *95*, 1892−1905.
(24) Wanigarathna, D. K. J. A.; Gao, J.; Liu, B. Fluorocarbon Separation in a Thermally Robust Zirconium Carboxylate Metal−Organic Framework. *Chem.—Asian J.* **2018**, *13*, 977−981.
(25) Wanigarathna, D. J. A.; Gao, J.; Takanami, T.; Zhang, Q.; Liu, B. Adsorption Separation of R-22, R-32 and R-125 Fluorocarbons using 4A Molecular Sieve Zeolite. *ChemistrySelect* **2016**, *1*, 3718−3722.
(26) Pardo, F.; Zarca, G.; Urtiaga, A. Separation of Refrigerant Gas Mixtures Containing R32, R134a, and R1234yf through Poly(ether-block-amide) Membranes. *ACS Sustainable Chem. Eng.* **2020**, *8*, 2548−2556.
(27) Pardo, F.; Zarca, G.; Urtiaga, A. Effect of feed pressure and long-term separation performance of Pebax-ionic liquid membranes for the recovery of difluoromethane (R32) from refrigerant mixture R410A. *J. Membr. Sci.* **2021**, *618*, 118744.
(28) Freire, M. G.; Neves, C. M. S. S.; Marrucho, I. M.; Coutinho, J. A. P.; Fernandes, A. M. Hydrolysis of tetrafluoroborate and hexafluorophosphate counter ions in imidazolium-based ionic liquids. *J. Phys. Chem. A* **2010**, *114*, 3744−3749.
(29) Xue, Z. Hydrolysis of Ionic Liquids. In *Encyclopedia of Ionic Liquids*; Zhang, S., Ed.; Springer Singapore: Singapore, 2019; pp 1−5.
(30) David, O. C.; Gorri, D.; Urtiaga, A.; Ortiz, I. Mixed gas separation study for the hydrogen recovery from H2/CO/N2/CO2 post combustion mixtures using a Matrimid membrane. *J. Membr. Sci.* **2011**, *378*, 359−368.
(31) Zarca, G.; Ortiz, I.; Urtiaga, A. Copper(I)-containing supported ionic liquid membranes for carbon monoxide/nitrogen separation. *J. Membr. Sci.* **2013**, *438*, 38−45.
(32) Zarca, G.; Ortiz, I.; Urtiaga, A. Facilitated-transport supported ionic liquid membranes for the simultaneous recovery of hydrogen and carbon monoxide from nitrogen-enriched gas mixtures. *Chem. Eng. Res. Des.* **2014**, *92*, 764−768.
(33) Tillner-Roth, R.; Yokozeki, A. An International Standard Equation of State for Difluoromethane (R-32) for Temperatures from the Triple Point at 136.34 K to 435 K and Pressures up to 70 MPa. *J. Phys. Chem. Ref. Data* **1997**, *26*, 1273−1328.
(34) Tillner-Roth, R.; Baehr, H. D. An International Standard Formulation for the Thermodynamic Properties of 1,1,1,2-Tetrafluoroethane (HFC-134a) for Temperatures from 170 K to 455 K and Pressures up to 70 MPa. *J. Phys. Chem. Ref. Data* **1994**, *23*, 657−729.
(35) Richter, M.; McLinden, M. O.; Lemmon, E. W. Thermodynamic Properties of 2,3,3,3-Tetrafluoroprop-1-ene (R1234yf): Vapor Pressure and p−ρ−T Measurements and an Equation of State. *J. Chem. Eng. Data* **2011**, *56*, 3254−3264.
(36) Chen, H. Z.; Li, P.; Chung, T.-S. PVDF/ionic liquid polymer blends with superior separation performance for removing CO2 from hydrogen and flue gas. *Int. J. Hydrogen Energy* **2012**, *37*, 11796−11804.
(37) Li, P.; Paul, D. R.; Chung, T.-S. High performance membranes based on ionic liquid polymers for CO2 separation from the flue gas. *Green Chem.* **2012**, *14*, 1052−1063.
(38) Ribeiro, C. P.; Freeman, B. D. Sorption, Dilation, and Partial Molar Volumes of Carbon Dioxide and Ethane in Cross-Linked Poly(ethylene oxide). *Macromolecules* **2008**, *41*, 9458−9468.
(39) Bernardo, P.; Jansen, J. C.; Bazzarelli, F.; Tasselli, F.; Fuoco, A.; Friess, K.; Izák, P.; Jarmarová, V.; Kačírková, M.; Clarizia, G. Gas transport properties of Pebax/room temperature ionic liquid gel membranes. *Sep. Purif. Technol.* **2012**, *97*, 73−82.
(40) Li, M.; Zhang, X.; Zeng, S.; Bai, L.; Gao, H.; Deng, J.; Yang, Q.; Zhang, S. Pebax-based composite membranes with high gas transport properties enhanced by ionic liquids for CO2 separation. *RSC Adv.* **2017**, *7*, 6422−6431.
(41) Rabiee, H.; Ghadimi, A.; Mohammadi, T. Gas transport properties of reverse-selective poly(ether-b-amide6)/[Emim][BF4] gel membranes for CO2/light gases separation. *J. Membr. Sci.* **2015**, *476*, 286−302.
(42) Ren, W.; Scurto, A. M. Phase equilibria of imidazolium ionic liquids and the refrigerant gas, 1,1,1,2-tetrafluoroethane (R-134a). *Fluid Phase Equilib.* **2009**, *286*, 1−7.
(43) Shiflett, M. B.; Harmer, M. A.; Junk, C. P.; Yokozeki, A. Solubility and Diffusivity of Difluoromethane in Room-Temperature Ionic Liquids. *J. Chem. Eng. Data* **2006**, *51*, 483−495.

https://doi.org/10.1021/acssuschemeng.1c00668
ACS Sustainable Chem. Eng. 2021, 9, 7012−7021

(44) Fraga, S. C.; Monteleone, M.; Lanč, M.; Esposito, E.; Fuoco, A.; Giorno, L.; Pilnáček, K.; Friess, K.; Carta, M.; McKeown, N. B.; Izák, P.; Petrusová, Z.; Crespo, J. G.; Brazinha, C.; Jansen, J. C. A novel time lag method for the analysis of mixed gas diffusion in polymeric membranes by on-line mass spectrometry: Method development and validation. *J. Membr. Sci.* **2018**, *561*, 39−58.
(45) Prabhakar, R. S.; Raharjo, R.; Toy, L. G.; Lin, H.; Freeman, B. D. Self-Consistent Model of Concentration and Temperature Dependence of Permeability in Rubbery Polymers. *Ind. Eng. Chem. Res.* **2005**, *44*, 1547−1556.
(46) Simari, C.; Nicotera, I.; Perrotta, I. D.; Clarizia, G.; Bernardo, P. Microscopic and macroscopic investigation on the gas diffusion in poly(ether-block-amide) membranes doped with polysorbate non-ionic surfactants. *Polymer* **2020**, *209*, 122949.
(47) Martins, A. P. S.; Fdz De Añastro, A.; Olmedo-Martínez, J. L.; Nabais, A. R.; Neves, L. A.; Mecerreyes, D.; Tomé, L. C. Influence of Anion Structure on Thermal, Mechanical and CO2 Solubility Properties of UV-Cross-Linked Poly(ethylene glycol) Diacrylate Iongels. *Membranes* **2020**, *10*, 46.
(48) Petropoulos, J. H. Mechanisms and theories for sorption and diffusion of gases in polymers. In *Polymeric Gas Separation Membranes*; Paul, D. R., Yampolskii, Y. P., Eds.; Taylor & Francis Group, 2017.
(49) Mateucci, S.; Yampolskii, Y. P.; Freeman, B. D.; Pinnau, I. Transport of Gases and Vapors in Glassy and Rubbery Polymers. In *Materials Science of Membranes for Gas and Vapor Separation*; Yampolskii, Y. P., Pinnau, I., Freeman, B. D., Eds.; John Wiley & Sons, 2006; pp 1−47.
(50) Prabhakar, R. S.; De Angelis, M. G.; Sarti, G. C.; Freeman, B. D.; Coughlin, M. C. Gas and Vapor Sorption, Permeation, and Diffusion in Poly(tetrafluoroethylene-co-perfluoromethyl vinyl ether). *Macromolecules* **2005**, *38*, 7043−7055.
(51) Cen, Y.; Staudt-Bickel, C.; Lichtenthaler, R. N. Sorption properties of organic solvents in PEBA membranes. *J. Membr. Sci.* **2002**, *206*, 341−349.
(52) Potreck, J.; Nijmeijer, K.; Kosinski, T.; Wessling, M. Mixed water vapor/gas transport through the rubbery polymer PEBAX 1074. *J. Membr. Sci.* **2009**, *338*, 11−16.
(53) Ghadimi, A.; Norouzbahari, S.; Vatanpour, V.; Mohammadi, F. An Investigation on Gas Transport Properties of Cross-Linked Poly(ethylene glycol diacrylate) (XLPEGDA) and XLPEGDA/TiO2 Membranes with a Focus on CO2 Separation. *Energy Fuels* **2018**, *32*, 5418−5432.
(54) Stern, S. A.; Fang, S.-M.; Frisch, H. L. Effect of pressure on gas permeability coefficients. A new application of "free volume" theory. *J. Polym. Sci., Polym. Phys. Ed.* **1972**, *10*, 201−219.

https://doi.org/10.1021/acssuschemeng.1c00668
ACS Sustainable Chem. Eng. 2021, 9, 7012−7021